Three-body force effect on the neutron and proton spectral functions in asymmetric nuclear matter

Pei Wang[1,2,3] and Wei Zuo[1,4,*]

[1]*Institute of Modern Physics, Chinese Academy of Sciences, Lanzhou 730000, China*
[2]*School of Physical Science and Technology, Lanzhou University, Lanzhou 730000, China*
[3]*University of Chinese Academy of Sciences, Beijing 100049, China*
[4]*State Key Laboratory of Theoretical Physics, Institute of Theoretical Physics, Chinese Academy of Sciences, Beijing 100190, China*

(Received 24 March 2014; revised manuscript received 29 April 2014; published 27 May 2014)

We investigate the effect of microscopic three-body forces (TBFs) on the off-shell behavior of the neutron and proton mass operators $M^{\tau}(k,\omega) = V^{\tau}(k,\omega) + iW^{\tau}(k,\omega)$ in asymmetric nuclear matter within the framework of the extended Brueckner-Hartree-Fock approach. We adopt the Argonne V_{18} two-body potential supplemented with a microscopic TBF as the realistic nucleon-nucleon interaction. At high densities well above the normal nuclear matter density, the TBF turns out to affect significantly the off-shell behavior of both the proton and neutron mass operators. The neutron and proton spectral functions in asymmetric nuclear matter are calculated and discussed. At low densities around and below the normal density, the TBF effect on the spectral functions turns out to be negligibly weak. At high densities well above the saturation density, the TBF is shown to affect noticeably the neutron and proton spectral functions.

DOI: 10.1103/PhysRevC.89.054319 PACS number(s): 21.65.Cd, 21.30.Fe, 24.10.Cn, 21.45.Ff

I. INTRODUCTION

Nucleon-nucleon (NN) correlations and their isospin dependence in asymmetric nuclear matter are of great interest since they are closely related to the structure of neutron-rich nuclei [1], particle production in heavy-ion collisions [2], and neutron-star physics [3]. The many-body NN correlations among nucleons can be directly reflected in the neutron and proton spectral functions [4], and the latter may play an important role in understanding the nature of the NN correlations, especially the short-range and tensor correlations in asymmetric nuclear matter [1].

The nucleon spectral function $S(k,\omega)$ describes the probability of removing a particle with momentum k from a target nuclear system, leaving the final system with an excitation energy ω. Experimentally, the information of $S(k,\omega)$ can be extracted from the high-resolution electron-scattering experiments [5–11] and the proton-induced knockout reactions [12–15]. These experiments have been performed on various nuclei with different values of the neutron to proton ratio N/Z, which not only clarify the limitation of the physical picture of independent particle motion in the standard mean-field theory, but also may lead to further insight into the isospin-dependence of NN correlations. Theoretically, the neutron and proton spectral functions have been investigated in asymmetric nuclear matter by using various microscopic nuclear many-body approaches, such as the relativistic Dirac-Brueckner-Hartree-Fock (DBHF) theory [16], the transport model [17], the in-medium T-matrix approach [18], the self-consistent Green's function method [13,19–21], and the Brueckner-Hartree-Fock (BHF) approach by including the hole-hole contribution [22]. Recently, the nucleon spectral function and the nucleon momentum distribution are calculated in finite nuclei within the framework of the Green's function theory [13,23–25] and the nonrelativistic many-body Schrödinger equation [26]. The obtained results have been shown to be useful for understanding the isospin dependence of NN correlations observed in the scattering experiments [6–9].

It is well known that the TBF is necessary for reproducing the empirical saturation properties of symmetric nuclear matter and for better describing the single-particle properties in the nonrelativistic microscopic BHF approach [27,28]. The TBF effect on the spectral function and nucleon momentum distribution has been investigated within the in-medium T-matrix method using the Urbana TBF [29], and the calculations are restricted to symmetric and pure neutron matter. For the symmetric case, the TBF effect turns out to be neglected at low densities (for example at the saturation density $\rho = 0.17$ fm^{-3}), while it becomes noticeable and induces an extra short-range correlation at high densities. This result is confirmed by our recent investigation of Ref. [30] within the framework of the extended BHF approach by adopting the Argonne $V_{18}(AV_{18})$ two-body interaction supplemented with a microscopic TBF. In the present work, we shall extend our previous investigation of Ref. [30] to asymmetric nuclear matter. We calculate the the neutron and proton off-shell mass operators and the spectral functions in asymmetric nuclear matter within the framework of the extended BHF approach. Especially, we pay special attention on the discussion of the TBF effect.

The TBF adopted in the present calculation is a microscopic TBF, and has been constructed in Refs. [27,28] by using the meson-exchange current approach. In this TBF model, the four most important mesons π, ρ, σ, and ω are considered. The TBF contains the contributions from various intermediate virtual processes such as virtual nucleon-antinucleon pair excitations, and nucleon resonances [28]. The parameters of the TBF model, i.e., the coupling constants and the form factors, are determined self-consistently by the corresponding two-body force within the one-boson-exchange potential (OBEP) model so that no adjustable parameters are introduced. The

*zuowei@impcas.ac.cn

components of the microscopic TBF model associated to the π and ρ meson exchanges have been developed for a long period by several authors [31–37]. The extension to include the σ and ω exchanges as well as the associated virtual nucleon-antinucleon pair excitations and nucleon resonances has been done by Grange *et al.* [28]. Further improvement of the TBF model has been achieved in Ref. [27] where new parameters of the TBF have been obtained self-consistently to reproduce the AV_{18} two-body interaction. It has been shown that the TBF leads to a significant improvement of the predicted saturation density and energy from (0.265 fm^{-3}, 18.25 MeV) to (0.198 fm^{-3}, 15.05 MeV) [27]. For more details, we refer to Refs. [27,28].

The present paper is organized as follows. In Sec. II, we provide a brief review of the adopted theoretical approaches including the extended BHF theory and the microscopic TBF model. We also give a definition and the corresponding physical interpretation of the mass operator and spectral function, as presented in Refs. [30,38]. In Sec. III, the calculated real and imaginary parts of the neutron and proton off-shell mass operators are reported and discussed. In Sec. IV, we calculate the neutron and proton spectral functions and investigate the TBF effect on their energy dependence. Finally, a summary is given in Sec. V.

II. FORMALISM

A. Brueckner theory with a microscopic TBF

Our calculations are based on the Brueckner theory extended to asymmetric nuclear matter [39]. The basic ingredient of the Brueckner theory is the in-medium two-body reaction matrix G, which in the case of asymmetric nuclear matter depends on the isospin components of the two colliding nucleons. The G matrix satisfies the isospin dependent Bethe-Goldstone (BG) equation [40,41],

$$G(\rho,\beta;\omega) = V_{NN} + V_{NN} \times \sum_{k_1k_2} \frac{|k_1k_2\rangle\, Q(k_1,k_2)\langle k_1k_2|}{\omega - \epsilon(k_1) - \epsilon(k_2) + i\eta} G(\rho,\beta;\omega), \quad (1)$$

where $k_i \equiv \{\vec{k}_i,\sigma_i,\tau_i\}$ denotes the single-particle (SP) momentum, the z components of spin and isospin of a nucleon, respectively. V_{NN} is the bare NN interaction, and ω is starting energy. The asymmetry parameter β is defined as $\beta = (\rho_n - \rho_p)/\rho$, where ρ_n, ρ_p and $\rho = \rho_p + \rho_n$ denote the neutron, proton, and total nucleon number densities, respectively. $Q(k_1,k_2) = [1 - n(k_1)][1 - n(k_2)]$ is the Pauli operator, which prevents the two intermediate nucleons from being scattered into their respective Fermi seas. Here, $n(k)$ is the Fermi distribution function, and it is given by the step function $\theta(k - k_F^\tau)$ at zero temperature. The proton ($\tau = p$) and neutron ($\tau = n$) Fermi momenta k_F^p and k_F^n are related to their corresponding densities ρ_p and ρ_n by the relations $k_F^p \equiv [\frac{3\pi^2}{2}(1-\beta)\rho]^{1/3}$ and $k_F^n \equiv [\frac{3\pi^2}{2}(1+\beta)\rho]^{1/3}$. $\epsilon(k)$ is the SP energy given by

$$\epsilon(k) = \frac{\hbar^2k^2}{2m} + U(k). \quad (2)$$

The convergence rate of the hole-line expansion depends on the choice of the auxiliary potential $U(k)$ [40–42]. Here, we adopt the continuous choice since it provides a much faster convergence of the hole-line expansion than the gap choice [43]. Under the continuous choice, the SP potential $U(k)$ describes physically at the lowest BHF level the nuclear mean field felt by a nucleon in nuclear medium [44] and is calculated from the real part of the on-shell G matrix:

$$U(k) = \mathrm{Re} \sum_{k' \leqslant k_F} \langle kk'|G[\rho,\epsilon(k) + \epsilon(k')]|kk'\rangle_A, \quad (3)$$

where the subscript A denotes antisymmetrization of the matrix elements. The coupled equations (1)–(3) have to be solved in a self-consistent way.

The realistic NN interaction V_{NN} is a basic input of the BG equation. In the present calculation, we adopt the AV_{18} two-body interaction [45] plus a microscopic TBF [27] as our realistic NN interaction. As already mentioned in the introduction, the adopted TBF model is based on the meson exchange current approach [27,28,33]. The parameters (the meson-nucleon couplings and form factors) in this TBF model have been self-consistently determined to reproduce the AV_{18} two-body force using the OBEP approximation, and their values can be found in Ref [27].

Recently, in Refs. [48,49], a self-consistent scheme has been developed to include a TBF in the Green's function approach, and the properties of symmetric nuclear matter have been calculated by adopting the chiral two-body and three-body interactions. The authors in these papers have stressed that TBF at the one-body and two-body level has to be handled differently in order to get a consistency for including the TBF effect at the Hartree-Fock level and all the successive orders in the dispersive contributions. Within the framework of the Brueckner theory, a fully consistent treatment of the TBF requires us to consider the three-body Faddeev problem. To avoid the complication of the in-medium three-body Faddeev problem, an approximation scheme has been devised to reduce the TBF to an equivalent two-body force [28] based on the solution of the Bethe-Faddeev equation valid for a strongly repulsive central two-body force [50]. This scheme consists in saturating the quantum numbers of the third nucleon properly weighted by means of the correlation wave functions with the two others, i.e., $\psi(r_{ij}) = 1 - g(r_{ij})$, g being the defect function. In the BHF approach, the TBF enters the BG equation only explicitly via the equivalent two-body force. The auxiliary potential in the BG equation plays the role in controlling the convergency of the hole-line expansion [40] and the TBF affects the auxiliary potential only implicitly via the G matrix during the self-consistent iteration procedure for solving the BG equation. The consistency of inclusion the TBF at the one-body and two-body levels in the BHF calculation is only partly kept, and the price paid is that a number of successive approximations have been made to get the equivalent two-body force by averaging the TBF, especially the double-exchange diagrams are neglected. The above approximation has been extensively applied in the BHF calculations for including TBF contribution, and its justification can be found in Refs. [28,33–36,46,47]. In this averaging scheme, the direct

and most important single-exchange TBF contributions are taken into account. The missing contributions, especially from the double-exchange diagrams, have been shown to be about 20% [33–36]. Accordingly, the above scheme has been thought reasonable. Going beyond this approximation for including TBF in the Brueckner theory requires a big effort and need to be done in the future.

In r space, the equivalent two-body force reduced from the TBF by averaging over the third nucleon degree of freedom can be written as [27,28],

$$\overline{V}_{ij}(r) = \rho \int d^3r_k \sum_{\sigma_k,\tau_k} [1 - g(r_{ik})]^2 [1 - g(r_{jk})]^2 V_{ijk}, \quad (4)$$

where $g(r)$ is the defect function, which reflects the nucleon-nucleon correlations in medium [28,51]. Equations (1)–(4) are coupled with each other, and need to be solved self-consistently.

In this work, the calculation has been performed by including a large number of partial waves ($J_{\max} = 9$) in the expansion of the G matrix, and by using a large momentum cutoff ($k_{\max} = 5\,\mathrm{fm}^{-1}$) in the self-consistent auxiliary SP potential $U(k)$. For the sake of simplification in calculation, the angle-average approximation for the Pauli operator and energy denominator have been adopted in Eq. (1) [52].

B. Mass operator and spectral function in asymmetric nuclear matter

One of the main purposes of the present work is to explore the off-shell behavior of the neutron and proton mass operators in asymmetric nuclear matter. In the spirit of the Brueckner-Bethe-Goldstone theory, the mass operator $M^\tau(k,\omega)$ can be expanded in a perturbation series according to the number of hole lines as demonstrated in Refs. [41,42,53]. In the expansion of mass operator [42], the first two terms $M^\tau(k,\omega) = M_1^\tau(k,\omega) + M_2^\tau(k,\omega)$ have been taken into account in the present calculation. The lowest-order term $M_1^\tau(k,\omega)$ is the standard BHF SP potential. The second-order term $M_2^\tau(k,\omega)$ is called the Pauli rearrangement term and it describes the effect of the ground-state two-hole correlations on the SP potential [54]. Their expressions are given as follows:

$$\begin{aligned} M_1^\tau(k,\omega) &\equiv \sum_{\tau'} M_1^{\tau\tau'}(k,\omega) \\ &= \sum_{\tau'} \sum_{h<k_F^{\tau'}} \langle kh|G^{\tau\tau'}[\omega + \epsilon^{\tau'}(h)]|kh\rangle_A, \end{aligned} \quad (5)$$

$$\begin{aligned} M_2^\tau(k,\omega) &\equiv \sum_{\tau'} M_2^{\tau\tau'}(k,\omega) = \frac{1}{2} \sum_{\tau'} \sum_{n>k_F^{\tau'}} \sum_{l<k_F^\tau} \sum_{m<k_F^{\tau'}} \\ &\times \frac{|\langle lm|G^{\tau\tau'}[\epsilon^\tau(l) + \epsilon^{\tau'}(m)]|kn\rangle_A|^2}{\omega + \epsilon^{\tau'}(n) - \epsilon^\tau(l) - \epsilon^{\tau'}(m) - i\eta}. \end{aligned} \quad (6)$$

The mass operator $M^\tau(k,\omega)$ is a complex quantity, i.e., $M^\tau(k,\omega) = V^\tau(k,\omega) + iW^\tau(k,\omega)$. The real and imaginary parts of the mass operator are connected by the dispersion relation [38]. The off-shell behavior of the mass operator, i.e., its dependence on momentum $\vec{k}$ and energy ω, can be calculated according to Eqs. (5) and (6) as long as the G matrix is obtained.

The neutron and proton quasiparticle (QP) energies ε_{QP}^τ are given by the self-consistent solution of the following energy-momentum relation,

$$\varepsilon_{QP}^\tau(k) = \frac{\hbar^2 k^2}{2m} + V^\tau\left[k, \varepsilon_{QP}^\tau(k)\right]. \quad (7)$$

The on-shell mass operator $M^\tau(k,\omega)$ is calculated by setting $\omega = \varepsilon_{QP}^\tau$ in the mass operator, and its real part can be identified as the potential energy felt by a neutron or a proton with momentum $\vec{k}$ in asymmetric nuclear matter. Using the Lehmann representation for the Green's function $G^\tau(k,\omega) = [\omega - k^2/2m - M^\tau(k,\omega)]^{-1}$, the neutron and proton spectral functions can be expressed in terms of the mass operator, i.e.,

$$S^\tau(k,\omega) = -\frac{1}{\pi} \frac{W^\tau(k,\omega)}{[\omega - k^2/2m - V^\tau(k,\omega)]^2 + [W^\tau(k,\omega)]^2}, \quad (8)$$

with the sum rule

$$\int_{-\infty}^{\infty} S^\tau(k,\omega)\, d\omega = 1. \quad (9)$$

The neutron and proton occupation probabilities $n^\tau(k)$ are related to their spectral functions by the following two equations:

$$n^\tau(k) = \int_{-\infty}^{\omega_F^\tau} S^\tau(k,\omega)\, d\omega, \quad (10)$$

and

$$n^\tau(k) = 1 - \int_{\omega_F^\tau}^{\infty} S^\tau(k,\omega)\, d\omega, \quad (11)$$

where $\omega_F^\tau = \varepsilon_{QP}^\tau(k_F^\tau)$ is the Fermi energy. For a system with A nucleons, $S^\tau(k,\omega)$ measures the probability density of finding the residual $(A-1)$ nucleon system with an excitation energy of $E^* = \omega_F^\tau - \omega$ $(\omega < \omega_F^\tau)$ after removing a nucleon with momentum k from the ground state, or the probability density of finding the residual $(A+1)$ nucleon system with $E^* = \omega - \omega_F^\tau$ $(\omega > \omega_F^\tau)$ by adding a nucleon to the ground state.

As a function of ω, $S^\tau(k,\omega)$ behaves like a δ function near the Fermi energy ω_F^τ, and its energy dependence becomes rather flat in the energy region away from the Fermi energy. In order to obtain accurately the spectral distribution around the Fermi energy, the present calculations have been performed by using two different mesh sizes in different energy regions, i.e., a small mesh size of $\Delta\omega = 0.5\,\mathrm{MeV}$ in the region of $\omega_F^\tau - 50\,\mathrm{MeV} < \omega < \omega_F^\tau + 50\,\mathrm{MeV}$, and a large one of 5 MeV for the regions of $\omega > \omega_F^\tau + 50\,\mathrm{MeV}$ and $\omega < \omega_F^\tau - 50\,\mathrm{MeV}$. The numerical stability and accuracy have been checked to be satisfactory.

III. OFF-SHELL PROPERTIES OF THE NEUTRON AND PROTON MASS OPERATOR AT FIXED MOMENTUM

A. Imaginary part of the off-shell mass operator

The imaginary part of mass operator determines how the QP strength and lifetime are modified in nuclear medium from the noninteracting Fermi gas. In Fig. 1, we display the energy $(\omega - e_F)$ dependence of $W^\tau(k,\omega) = W_1^\tau(k,\omega) + W_2^\tau(k,\omega)$ for

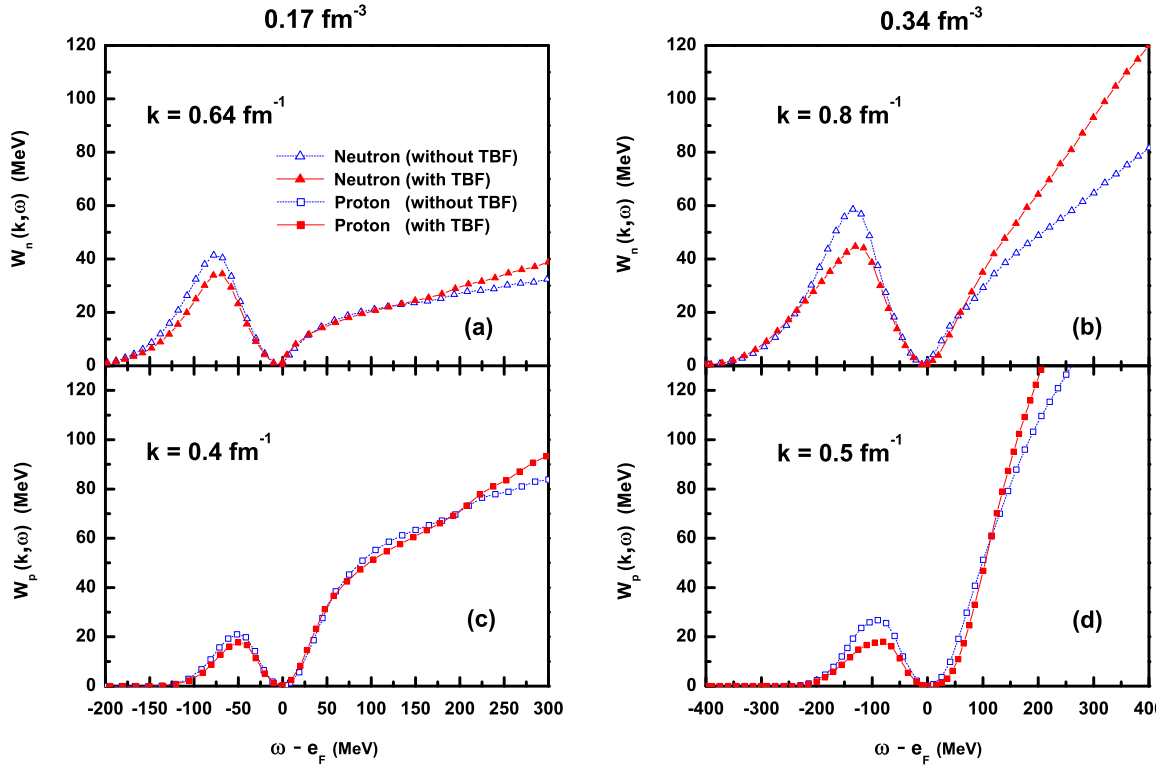

FIG. 1. (Color online) Dependence of $W^\tau(k,\omega) = W_1^\tau(k,\omega) + W_2^\tau(k,\omega)$ on $\omega - e_F$ for a fixed momentum of $k = 0.4k_F^\tau$ in asymmetric nuclear matter at a asymmetry of $\beta = 0.6$ and two densities of $\rho = 0.17$ fm^{-3} (left panels) and $\rho = 0.34$ fm^{-3} (right panels). The upper panels refer to neutron, and the lower ones to proton. The curves with filled squares and filled triangles are obtained by including the TBF contribution.

proton and neutron in asymmetric nuclear matter at a given asymmetry of $\beta = 0.6$ for two densities of $\rho = 0.17$ fm^{-3} and $\rho = 0.34$ fm^{-3}, respectively. $W_1^\tau(k,\omega)$ and $W_2^\tau(k,\omega)$ are given by $W_1^\tau(k,\omega) = \mathrm{Im}\, M_1^\tau(k,\omega)$ and $W_2^\tau(k,\omega) = \mathrm{Im}\, M_2^\tau(k,\omega)$. In Fig. 1, the results are given at a fixed momentum of $k = 0.4k_F^\tau$. The e_F^τ is the proton or neutron Fermi energy in the BHF approximation: $e_F^\tau = \epsilon(k_F^\tau) = k_F^{\tau 2}/2m + U_{\mathrm{BHF}}^\tau(k_F^\tau)$. In analogy with the case of symmetric matter [30,38], the contributions to $W^\tau(k,\omega)$ in the energy region of $\omega < e_F^\tau$ originate from the rearrangement terms $W_2^\tau(k,\omega)$ of the proton and neutron mass operators, while those at energies of $\omega > e_F^\tau$ come from the first-order terms $W_1^\tau(k,\omega)$. One important feature in asymmetric nuclear matter is that the magnitude of $W_2^\tau(k,\omega)$ is larger for neutron (upper panels) than that for proton (lower panels) in the region of $\omega < e_F^\tau$. The difference between the proton and neutron mass operators can be readily understood according to the isospin-asymmetry dependence of the tensor correlation effect in the proton-neutron interaction. The above result is in agreement with the prediction within the framework of the self-consistent Green's function method in Ref. [55], where the effect of the isospin $T = 0$ tensor SD coupled channel on the imaginary part of self-energy has been clarified. On the other hand, the quantity $W_1^\tau(k,\omega)$ turns out to be larger in magnitude for proton than that for neutron, and its magnitude increases monotonically as a function of energy ω in the region of $\omega > e_F^\tau$. This result also reflects the fact that the isospin $T = 0$ SD tensor component induces a strong short-range correlation (SRC) in asymmetric nuclear matter, which is consistent with the results obtained by using the framework of the Green function approach in Ref. [56] and the extended BHF approach in Ref. [57]. The TBF effect on the ω dependence of $W^\tau(k,\omega)$ is also reported in Fig. 1. By comparing the open symbols with the corresponding filled symbols in Fig. 1, it is seen that the TBF effect is to decrease the magnitudes of $W_2^\tau(k,\omega)$ for both proton and neutron below their respective Fermi energies. At the high density of $\rho = 0.34$ fm^{-3} (right panels), the reduction of the magnitude of $W_2^\tau(k,\omega)$ due to the TBF effect turns out to be more pronounced in the region of $\omega < e_F^\tau$ as compared with that at the empirical saturation density $\rho_0 = 0.17$ fm^{-3} (left panels). In the energy region of $\omega > e_F^\tau$, the TBF effect is negligibly small at the saturation density $\rho_0 = 0.17$ fm^{-3}. At the high density of $\rho = 0.34$ fm^{-3}, the TBF effect is shown to become noticeable, and it leads to a faster increasing of the magnitude of $W_1^\tau(k,\omega)$ as a function of ω for $\omega > 110$ MeV. It is clearly seen that inclusion of the TBF may induce an extra SRC, and consequently leads to larger scattering amplitudes in particle-particle states in dense nuclear medium as compared with the case of excluding the TBF. It is worth noticing that, in asymmetric matter (for example $\beta = 0.6$), the TBF has a stronger effect to decrease the magnitudes of $W_2^\tau(k,\omega)$ for both proton and neutron as compared with the result for symmetric matter [30]. As a result, the TBF effect may depend sensitively on the isospin asymmetry β, in agreement with the previous studies [27].

B. Real part of the off-shell mass operator

Figure 2 shows the real parts of the proton and neutron mass operators $V^\tau(k,\omega) = V_1^\tau(k,\omega) + V_2^\tau(k,\omega)$ vs. $(\omega - e_F^\tau)$

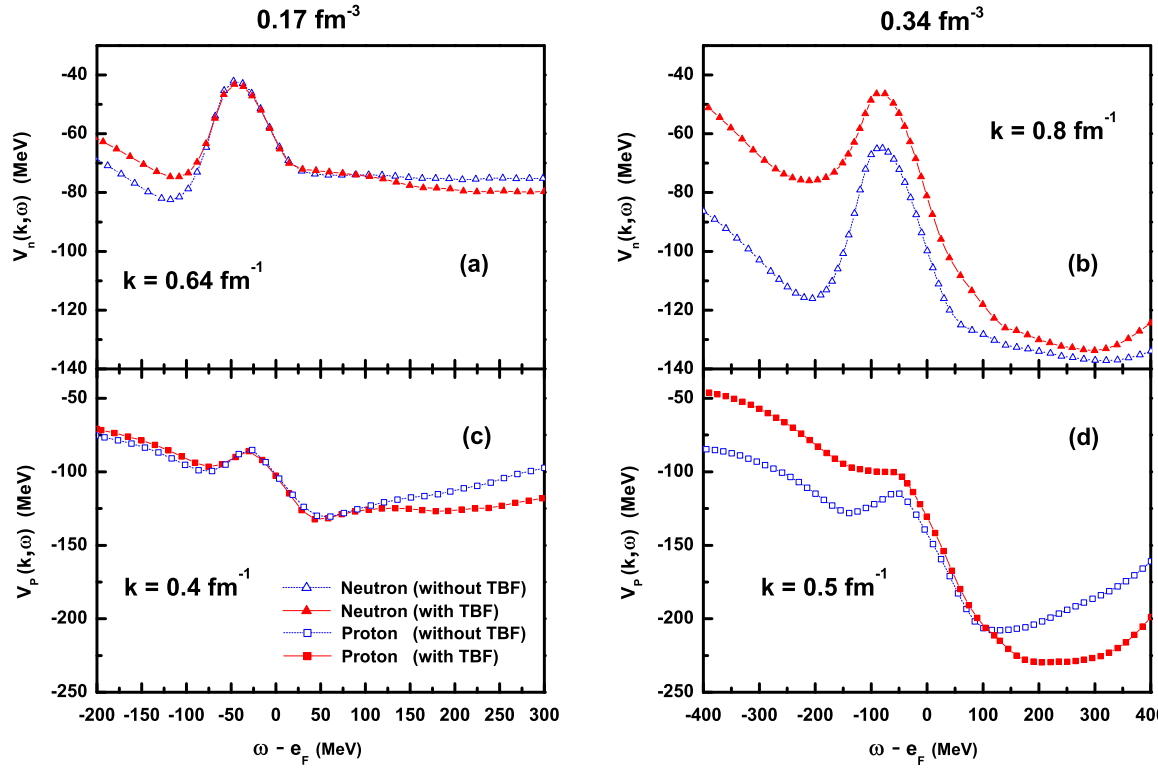

FIG. 2. (Color online) Dependence of $V^\tau(k,\omega) = V_1^\tau(k,\omega) + V_2^\tau(k,\omega)$ on $\omega - e_F$ for a fixed momentum of $k = 0.4k_F^\tau$ in asymmetric nuclear matter at a asymmetry of $\beta = 0.6$ and two densities of $\rho = 0.17$ fm^{-3} (left panels) and $\rho = 0.34$ fm^{-3} (right panels). The upper panels refer to neutron, and the lower ones to proton. The curves with filled squares and filled triangles are obtained by including the TBF contribution.

in asymmetric nuclear matter at $\beta = 0.6$ for two densities of $\rho = 0.17$ fm^{-3} and 0.34 fm^{-3}. The gross structure of the quantity $V^\tau(k,\omega)$ as a function of $(\omega - e_F)$ is determined to a large extent by the first-order term $V_1^\tau(k,\omega)$. The rearrangement contribution $V_2^\tau(k,\omega)$ is repulsive and it reduces the attraction of the BHF mean field $V_1^\tau(k,\omega)$ in the energy region of $-100 < \omega - e_F^\tau < 30$ MeV ($-200 < \omega - e_F^\tau < 50$ MeV) for the density $\rho = 0.17$ fm^{-3} ($\rho = 0.34$ fm^{-3}). The real parts of the proton and neutron mass operators $V^\tau(k,\omega)$ can be related to their imaginary parts $W^\tau(k,\omega)$ by using a dispersion relation [38]. As displayed in Fig. 2, the attraction of the $V^\tau(k,\omega)$ for proton in asymmetric nuclear matter is stronger than that for neutron, which is attributed to the fact that the attractive contribution of the $T = 0$ tensor SD coupled channel becomes more effective (less effective) on protons (neutrons) with increasing asymmetry β [39]. By comparing the left panels ($\rho = 0.17$ fm^{-3}) with the right ones ($\rho = 0.34$ fm^{-3}) in Fig. 2, one may notice that the overall energy dependence of $V_1^\tau(k,\omega)$ is weaker at the saturation density of $\rho = 0.17$ fm^{-3} than that at the density of $\rho = 0.34$ fm^{-3}, which is two times the saturation density. This result can be partly understood by the fact that the energy dependence of the imaginary part $W_1^\tau(k,\omega)$ is stronger at a higher density as shown in Fig. 1. The TBF effect on the predicted $V^\tau(k,\omega)$ is also displayed in Fig. 2. At the saturation density of $\rho = 0.17$ fm^{-3}, the TBF effect on $V^\tau(k,\omega)$ is relatively weak. Inclusion of the TBF in the calculation reduces the attraction of $V^\tau(k,\omega)$ in the energy region of $\omega < e_F$, whereas it enhances of the attraction of $V^\tau(k,\omega)$ for $\omega > e_F$. At densities well above the saturation density (for example, $\rho = 0.34$ fm^{-3}), the TBF effect turns out to become noticeably strong. As a result, inclusion of the TBF reduces significantly the attraction of the proton potential $V^p(k,\omega)$ at $\omega < e_F$, and it may even lead to an overall enhancement of the repulsion of the neutron potential $V^n(k,\omega)$ in the whole range of energy. Besides, the TBF-induced repulsive contribution to $V^\tau(k,\omega)$ depends on asymmetry β, and the TBF repulsion turns out to be larger in asymmetric nuclear matter as compared with that in symmetric matter reported in Ref. [30].

IV. SPECTRAL FUNCTION AND OCCUPATION PROBABILITIES

The real and imaginary parts of the mass operator in Fig. 1 and Fig. 2 can be used to determine the neutron and proton spectral functions via Eq. (8). When the imaginary part $W^\tau(k,\omega)$ is sufficiently small as compared with the real part $V^\tau(k,\omega)$, the energy dependence of the spectral function is dominated by the QP peak in the Landau theory of Fermi liquids and the spectral function can be described by the QP approximation. In the QP approximation, the neutron and proton spectral functions can be written as $S^\tau(k,\omega) = \delta[\omega - \varepsilon_{QP}^\tau(k)]$, where $\varepsilon_{QP}^\tau(k)$ is the QP energy defined in Eq. (7). In the present calculation, the spectral functions $S^\tau(k,\omega)$ display peaks for proton and neutron at their respective QP energies $\omega = \varepsilon_{QP}^\tau(k)$ at which the term $[\omega - k^2/2m - V^\tau(k,\omega)]$ in the denominator of Eq. (8) vanishes, i.e., the positions of the peaks in the spectral functions are determined by the real parts of the mass oper-

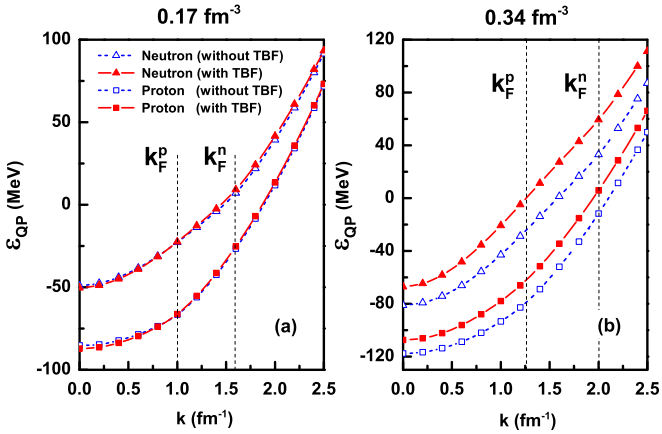

FIG. 3. (Color online) Proton and neutron quasiparticle energies vs momentum k ε^{τ}_{QP} in asymmetric nuclear matter at a asymmetry of $\beta = 0.6$ and two densities of $\rho = 0.17$ fm^{-3} (left panels) and $\rho = 0.34$ fm^{-3} (right panels), respectively. Filled symbols correspond to the results with the TBF contribution.

ators. At $\omega = \varepsilon^{\tau}_{QP}(k)$, the spectral functions are simplified as $S^{\tau}[k,\omega = \varepsilon^{\tau}_{QP}(k)] = -[\pi W^{\tau}(k,\omega = \varepsilon^{\tau}_{QP}(k))]^{-1}$, which implies the strengths of the peaks are determined by the imaginary parts of the mass operators. In Fig. 3, the neutron and proton QP energies $\varepsilon^{\tau}_{QP}(k)$ are reported as functions of momentum in asymmetric nuclear matter at $\beta = 0.6$. From Fig. 3, it is seen that the proton QP energy is more attractive than the neutron one since in neutron-rich matter, the SD tensor interaction felt by a neutron from the surrounding protons is weaker than that felt by a proton from the surrounding neutrons [39]. As a consequence, the peak locations in the proton and neutron spectral functions become different in asymmetric nuclear matter, and the peak in the neutron spectral function is located at a higher energy than the proton one. From Fig. 3 it is seen that at the saturation density of $\rho = 0.17$ fm^{-3} (left panel), the TBF effect is negligibly weak, while it gives an overall repulsive contribution to the proton and neutron QP energies $\varepsilon^{\tau}_{QP}(k)$ at the high density of $\rho = 0.34$ fm^{-3} (right panel). This implies that the TBF may shift the peak locations of the neutron and proton QP energies to higher energies, which is similar to the previous results in Refs. [29,30] for symmetric nuclear matter.

In Fig. 4, the neutron and proton spectral functions $S^{\tau}(k,\omega)$ in asymmetric matter at $\rho = 0.17$ fm^{-3} and $\beta = 0.6$ are displayed for two momenta of $k = 0.4k^{\tau}_F$ and $k = 1.5k^{\tau}_F$. In order to see more clearly the energy dependence and the peak locations of the spectral functions, respectively, the results are shown under the log coordinate in the left panels, and under the linear coordinate in the right panels. In asymmetric matter, the main difference of the spectral functions from the symmetric case comes from the isospin dependence of the mass operator and the separation of the neutron and proton Fermi surfaces. At $k = 0.4k^{\tau}_F$ (upper panels), the proton spectral function shows a more pronounced QP peak and a narrower distribution than the neutron one. This is partly due to the fact that the proton peak is closer to the Fermi surface as compared with the neutron one, and in agreement with the general expectation that the strength and lifetime of QP states increase strongly when the momenta k approach to the Fermi momentum k^{τ}_F. The main reason for the difference between the proton and neutron spectral functions can be traced back to the different

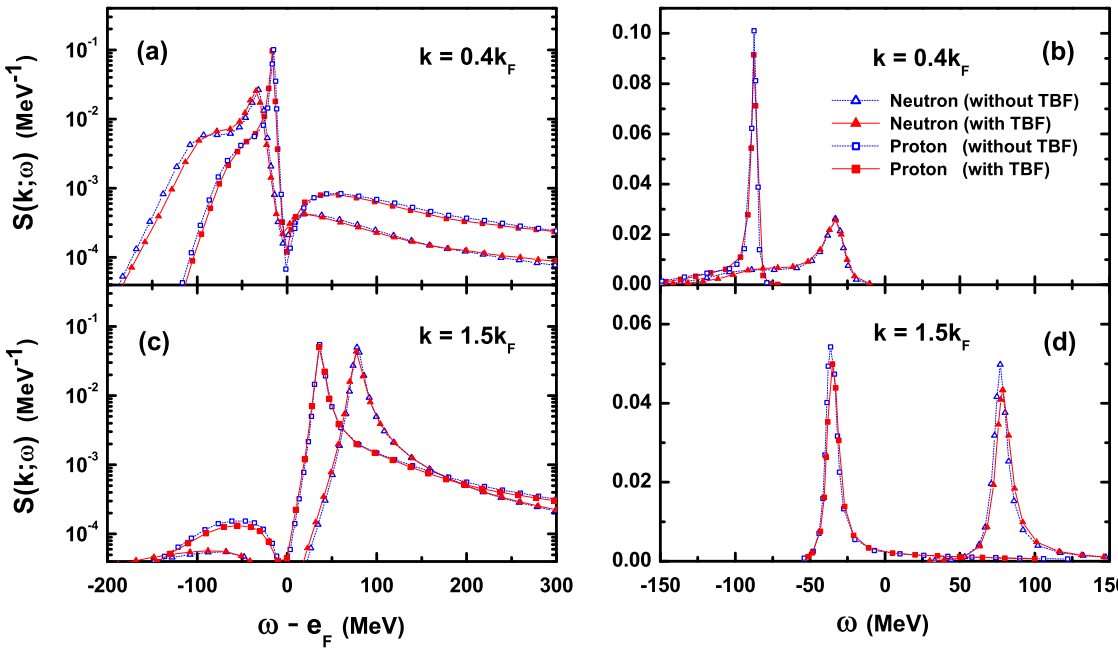

FIG. 4. (Color online) Neutron and proton spectral functions in asymmetric nuclear matter at $\beta = 0.6$ and $\rho = 0.17$ fm^{-3}, for two selected momenta of $k = 0.4k_F$ (upper panels) and $k = 1.5k_F$ (lower panels). The results are shown under the log coordinate in the left panels, and under the linear coordinate in the right panels. The filled symbols correspond to the results obtained by including the TBF contribution, while the open symbols are the results without the TBF.

imaginary parts $W_2^\tau(k,\omega)$ of the neutron and proton mass operators in the region of $\omega < e_F^\tau$. According to Eq. (8), the overall shapes of the spectral functions in the energy region of $\omega < e_F^\tau$ are determined to a large extent by the imaginary parts $W_2^\tau(k,\omega)$. The broader distribution of the neutron spectral function originates from a wider region of the nonvanishing $W_2^n(k,\omega)$ as compared to the proton one. On the other hand, the smaller imaginary part $W_2^p(k,\omega)$ leads to a larger peak in the proton spectral function than the neutron one, since the strengths of the peaks are inversely proportional to $W_2^\tau(k,\omega)$. At $k = 1.5k_F^\tau$ (lower panels), the proton spectral function is also larger than the neutron one in the region of $\omega < e_F^\tau$. At energies well above e_F^τ, it is noticed from the left panels of Fig. 4 that the proton spectral function has a larger high-energy tail than the neutron one, which is directly related to the strong neutron-proton SRC induced by the isospin $T = 0$ SD tensor component of NN interaction. Similar results have also been reported in Ref. [22] within the BHF approach by adopting the CD-Bonn potential, in Ref. [16] by using the DBHF approach, and in Ref. [17] within the framework of transport theory.

In Fig. 5, we show the neutron and proton spectral functions $S^\tau(k,\omega)$ in asymmetric nuclear matter at $\beta = 0.6$ and $\rho = 0.34$ fm^{-3}. In the figure, the filled symbols correspond to the result obtained by including the TBF contribution, while the open symbols are calculated by excluding the TBF. By comparing the filled symbols and the corresponding open symbols in Fig. 4, it is noticed that the TBF effect is negligibly small at the saturation density of $\rho = 0.17$ fm^{-3}. However, the TBF effect becomes noticeable at $\rho = 0.34$ fm^{-3}, which is well above the saturation density as shown in Fig. 5. From Fig. 5, it is shown that the TBF effect decreases slightly the background of the proton and neutron spectral functions (left panels) and leads to a shift of the peak locations to higher energies (right panels). This is readily understood since the TBF decreases the magnitude of the imaginary part of the mass operator, and gives an extra repulsive contribution to the real part, i.e. it may increase the neutron and proton QP energies. At energies of $\omega > e_F^\tau$, the TBF effect on the neutron and proton spectral functions are shown to be not so drastic as that on the mass operators. In the energy region well above e_F^τ, inclusion of the TBF is expected to lead to larger high-energy tails as compared with the case of not including the TBF, which may be regarded as a manifestation of the TBF effect on the NN correlations in the spectral functions. In order to test the numerical accuracy of the present work, the sum rule of the spectral function has been checked by performing the integration over ω in Eq. (9). In the present calculation, the neutron and proton spectral functions are calculated in the energy range of -400 MeV $< \omega < 400$ MeV. The integrations over ω from -400 MeV to 400 MeV are found to be about 0.93. According to Figs. 4 and 5, we expect the 7% deviation is due to the missing contribution of the high-energy tails in the region of $\omega > 400$ MeV. In order to include this contribution, we make a polynomial extrapolation to get the spectral functions in the region of $\omega > 400$ MeV according to the calculated ones in the region of $\omega < 400$ MeV. By using the calculated values in the region of $\omega < 400$ MeV and the extrapolation values in $\omega > 400$ MeV, the neutron and proton spectral functions are found to be almost exactly normalized [the integrations in Eq. (9) are about 0.99] in both cases of including and excluding the TBF. We also noticed that the TBF effect on the spectral function in pure neutron matter has been investigated in Ref. [29] using the in-medium T-matrix method with the Urbana TBF. The Urbana TBF may leads to

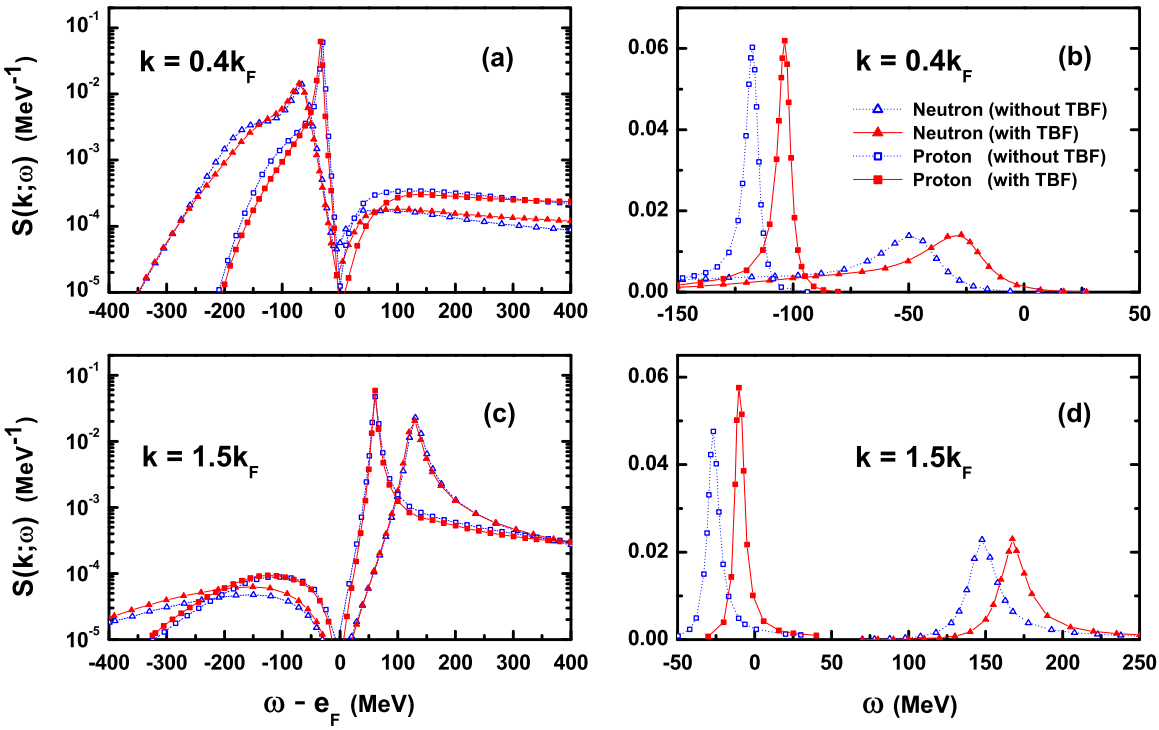

FIG. 5. (Color online) The same as Fig. 4, but the results are obtained at $\rho = 0.34$ fm^{-3}.

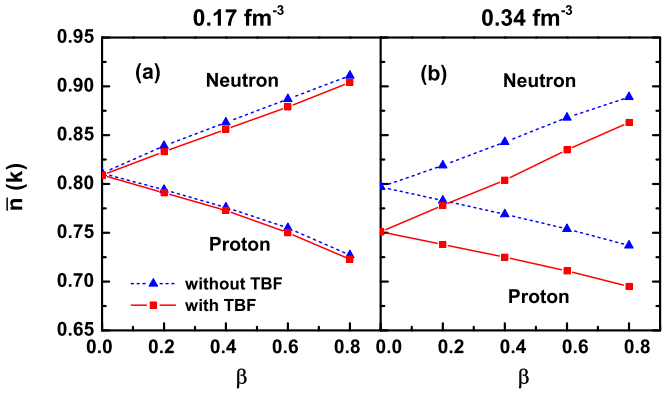

FIG. 6. (Color online) Averaged neutron and proton occupation probabilities inside their respective Fermi seas. The results are displayed as a function of isospin asymmetry β for two densities $\rho = 0.17\,\mathrm{fm}^{-3}$ (left panel) and $\rho = 0.34\,\mathrm{fm}^{-3}$ (right panel). The solid and dashed lines correspond to the two cases with and without the TBF contribution, respectively.

a shift of the peak location to slightly lower energy, because it gives an extra attractive contribution to the real part of the self-energy in pure neutron matter.

In order to check further the present calculations, in Fig. 6, we display the neutron and proton occupation probabilities $\overline{n}_\tau(k)$ averaged below their respective Fermi momenta $k < k_F^\tau$ in asymmetric matter at various asymmetries $\beta = 0, 0.2, 0.4, 0.6$, and 0.8 for two densities of $\rho = 0.17\ \mathrm{fm}^{-3}$ and $\rho = 0.34\ \mathrm{fm}^{-3}$. The results are obtained from Eq. (10) by averaging the neutron and proton momentum distribution $n_\tau(k)$ in their respective Fermi seas, respectively. In both cases of including and excluding the TBF, it is clearly seen that the averaged neutron and proton occupation probabilities depend sensitively on the isospin asymmetry β. In asymmetric nuclear matter, the averaged neutron occupation $\overline{n}_n(k)$ is shown to be larger than the proton occupation $\overline{n}_p(k)$, which is directly related to the fact that the proton spectral function has a larger high-energy tail than the neutron one below their respective Fermi momenta. $\overline{n}_n(k)$ turns out to increase linearly as a function of β, while $\overline{n}_p(k)$ decreases linearly as increasing β. The present results are compatible with the previous predictions reported in Refs. [20,57–61]. The averaged occupation probabilities in our present calculation are slightly larger than the results in Ref. [22] at the saturation density $\rho = 0.17\ \mathrm{fm}^{-3}$. The isospin dependence of $\overline{n}_\tau(k)$ may help us to understand the properties of short-range and tensor correlations in asymmetric nuclear matter [8,9,20,57]. Due to the strong $T = 0$ SD tensor component in neutron-proton interaction, increasing asymmetry β tends to widen the neutron spectral distribution in the energy region of $\omega < e_F^\tau$ and thus lead to an enhancement of the neutron occupation probability below its Fermi surface, whereas the proton occupation probability gets smaller at a higher asymmetry. The above result is understandable and reflects the effect of the strong neutron-proton correlations induced by the $T = 0$ SD tensor interaction. Similar results have been reported in Ref. [20] by using the self-consistent Green's function approach with various NN interactions, and in Ref. [57] by using the extended BHF approach with the AV_{18} potential. Their results confirm the important role played by the tensor force in determining the isospin dependence of the neutron and proton momentum distributions in asymmetric nuclear matter. The TBF effect on the isospin dependence of $\overline{n}_\tau(k)$ is also shown in Fig. 6. At the saturation density of $\rho = 0.17\ \mathrm{fm}^{-3}$ (left panel), the TBF effect on the neutron and proton averaged occupation probabilities $\overline{n}_n(k)$ and $\overline{n}_p(k)$ is negligibly small. Whereas, at $\rho = 0.34\ \mathrm{fm}^{-3}$ (right panel), the TBF effect may sizably affect the neutron and proton occupations. Inclusion of the TBF leads to an overall reduction of both $\overline{n}_n(k)$ and $\overline{n}_p(k)$ in the whole isospin-asymmetry range of $0 \leqslant \beta \leqslant 0.8$, in good agreement with the conclusion of Ref. [57].

V. CONCLUSIONS

In the present study, we have extended our previous work of Ref. [30] for symmetric nuclear matter and investigated the neutron and proton off-shell mass operators as well as the spectral functions in asymmetric nuclear matter within the framework of the extended BHF approach by using the AV_{18} two-body interaction supplemented with a microscopic TBF. The first two terms in the hole-line expansion of the mass operator have been taken into account. For a fixed momentum $k = 0.4k_F$ and asymmetry $\beta = 0.6$, the imaginary part $W^\tau(k,\omega)$ of the proton mass operator is shown to be smaller (larger) in the energy region of $\omega < e_F (\omega > e_F)$ than the neutron one. In the low-energy region of $\omega < e_F^\tau$, the predicted smaller proton $W^\tau(k,\omega)$, as compared with the neutron one, leads to a more pronounced QP peak in the proton spectral distribution and a larger depletion of the proton Fermi sea. In the energy region of $\omega > e_F^\tau$ the proton spectral function has a larger high-energy tail than the neutron one, which implies that at a higher asymmetry the SRC effect induced by the tensor component in NN interaction becomes stronger on protons as compared with that on neutrons. Our calculations indicate that the TBF effect on the neutron and proton spectral functions is negligibly weak at low densities around and below the nuclear saturation density $\rho = 0.17\ \mathrm{fm}^{-3}$. It becomes noticeable only at high densities well above the saturation density (for example, $\rho = 0.34\ \mathrm{fm}^{-3}$). In the low-energy region of $\omega < e_F$, inclusion of the TBF leads to an enhancement of the repulsion of the real parts $V^\tau(k,\omega)$ of the mass operators, while it reduces the magnitudes of the imaginary parts $W^\tau(k,\omega)$ for both proton and neutron. As a result, the TBF effect is expected to induce an extra SRC in dense nuclear medium, which shifts the peak locations in the neutron and proton spectral functions to higher energies. The present results also confirm the previous results concerning the isospin dependence of the neutron and proton occupation probabilities [20,22,60] and the TBF effect on the momentum distributions in asymmetric nuclear matter [57].

ACKNOWLEDGMENTS

The work is supported by the 973 Program of China (No. 2007CB815004), the National Natural Science Foundation of China (11175219), and the Knowledge Innovation Project (KJCX2-EW-N01) of Chinese Academy of Sciences.

[1] R. Schiavilla, R. B. Wiringa, S. C. Pieper, and J. Carlson, Phys. Rev. Lett. **98**, 132501 (2007).
[2] O. Buss, T. Gaitanos, K. Gallmeister, H. van Hees, M. Kaskulov, O. Lalakulich, A. B. Larionov, T. Leitner, J. Weil, and U. Mosel, Phys. Rep. **512**, 1 (2012).
[3] L. Frankfurt, M. Sargsian, and M. Strikman, Int. J. Mod. Phys. A **23**, 2991 (2008).
[4] W. H. Dickhoff, Phys. Rep. **242**, 119 (1994).
[5] G. van der Steenhoven, Nucl. Phys. A **527**, 17 (1991).
[6] J. Arrington, D. W. Higinbotham, G. Rosner, and M. Sargsian, Prog. Part. Nucl. Phys. **67**, 898 (2012).
[7] D. Rohe *et al.* (E97-006 Collaboration), Phys. Rev. Lett. **93**, 182501 (2004).
[8] D. Rohe, Eur. Phys. J. A **17**, 439 (2003).
[9] R. Subedi, R. Shneor, P. Monaghan *et al.*, Science **320**, 1476 (2008).
[10] I. Bobeldijk, H. P. Blok, H. B. van den Brink, G. E. Dodge, W. H. A. Hesselink, E. Jans, W-J. Kasdorp, L. Lapikás, J. J. van Leeuwe, C. Marchand, G. Onderwater, A. Pellegrino, M. van Sambeek, C. M. Spaltro, G. van der Steenhoven, J. J. M. Steijger, J. A. Templon, M. A. van Uden, R. de Vries, and P. K. A. de Witt Huberts, Phys. Lett. B **353**, 32 (1995); I. Bobeldijk *et al.*, Phys. Rev. Lett. **73**, 2684 (1994).
[11] L. Lapikás, J. Wesseling, and R. B. Wiringa, Phys. Rev. Lett. **82**, 4404 (1999).
[12] V. R. Pandharipande, I. Sick, and P. K. A. deWitt Huberts, Rev. Mod. Phys. **69**, 981 (1997).
[13] W. Dickhoff and C. Barbieri, Prog. Part. Nucl. Phys. **52**, 377 (2004).
[14] W. H. Dickhoff and M. Müther, Rep. Prog. Phys. **55**, 1947 (1992).
[15] R. Starink, M. F. van Batenburg, E. Cisbani, W. H. Dickhoff, S. Frullani, F. Garibaldi, C. Giusti, D. L. Groep, P. Heimberg, W. H. A. Hesselink, M. Iodice, E. Jans, L. Lapikás, R. De Leo, C. J. G. Onderwater, F. D. Pacati, R. Perrino, J. Ryckebusch, M. F. M. Steenbakkers, J. A. Templon, G. M. Urciuoli, and L. B. Weinstein, Phys. Lett. B **474**, 33 (2000).
[16] E. N. E. van Dalen and H. Müther, Phys. Rev. C **82**, 014319 (2010).
[17] P. Konrad, H. Lenske, and U. Mosel, Nucl. Phys. A **756**, 192 (2005).
[18] P. Bożek, Phys. Lett. B **586**, 239 (2004).
[19] T. Frick and H. Müther, Phys. Rev. C **68**, 034310 (2003); T. Frick, Kh. S. A. Hassaneen, D. Rohe, and H. Müther, *ibid.* **70**, 024309 (2004).
[20] A. Rios, A. Polls, and I. Vidana, Phys. Rev. C **79**, 025802 (2009); A. Rios, A. Polls, and W. H. Dickhoff, *ibid.* **79**, 064308 (2009).
[21] T. Frick, H. Müther, A. Rios, A. Polls, and A. Ramos, Phys. Rev. C **71**, 014313 (2005).
[22] Kh. S. A. Hassaneen and H. Müther, Phys. Rev. C **70**, 054308 (2004).
[23] H. Müther, A. Polls, and W. H. Dickhoff, Phys. Rev. C **51**, 3040 (1995); A. Polls, A. Ramos, C. C. Gearhart, W. H. Dickhoff, and H. Müther, Prog. Part. Nucl. Phys. **34**, 371 (1995).
[24] P. Fernández de Córdoba, E. Marco, H. Müther, E. Oset, and A. Faessler, Nucl. Phys. A **611**, 514 (1996).
[25] R. J. Charity, W. H. Dickhoff, L. G. Sobotka, and S. J. Waldecker, Eur. Phys. J. A **50**, 23 (2014).
[26] M. Alvioli, C. Ciofi degli Atti, L. P. Kaptari, C. B. Mezzetti, and H. Morita, Phys. Rev. C **87**, 034603 (2013); J. Mod. Phys. E **22**, 1330021 (2013).
[27] W. Zuo, A. Lejeune, U. Lombardo, and J.-F. Mathiot, Nucl. Phys. A **706**, 418 (2002); Eur. Phys. J. A **14**, 469 (2002).
[28] P. Grangé, A. Lejeune, M. Martzolff, and J.-F. Mathiot, Phys. Rev. C **40**, 1040 (1989).
[29] V. Somà and P. Bożek, Phys. Rev. C **78**, 054003 (2008).
[30] P. Wang, S. X. Gan, P. Yin, and W. Zuo, Phys. Rev. C **87**, 014328 (2013).
[31] B. Loiseau, Y. Nogami, and C. K. Ross, Nucl. Phys. A **165**, 601 (1971).
[32] M. Martzolff and P. Grange, Phys. Lett. B **92**, 46 (1980).
[33] S. A. Coon, M. D. Scadron, P. C. McNamee, B. R. Barrett, D. W. E. Blatt, and B. H. J. McKellar, Nucl. Phys. A **317**, 242 (1979).
[34] S. A. Coon and W. Glöckle, Phys. Rev. C **23**, 1790 (1981).
[35] S. A. Coon and M. T. Peña, Phys. Rev. C **48**, 2559 (1993).
[36] R. G. Ellis, S. A. Coon, and B. H. J. McKellar, Nucl. Phys. A **438**, 631 (1985).
[37] A. Stadler, J. Adam, H. Henning, and P. U. Sauer, Phys. Rev. C **51**, 2896 (1995).
[38] M. Baldo, I. Bombaci, G. Giansiracusa, U. Lombardo, C. Mahaux, and R. Sartor, Nucl. Phys. A **545**, 741 (1992).
[39] W. Zuo, I. Bombaci, and U. Lombardo, Phys. Rev. C **60**, 024605 (1999).
[40] B. D. Day, Rev. Mod. Phys. **50**, 495 (1978).
[41] M. Baldo, *Nuclear Methods and the Nuclear Equation of State* (World Scientific, Singapore, 1999).
[42] J. P. Jeukenne, A. Lejeune, and C. Mahaux, Phys. Rep. **25**, 83 (1976).
[43] H. Q. Song, M. Baldo, G. Giansiracusa, and U. Lombardo, Phys. Rev. Lett. **81**, 1584 (1998); M. Baldo, A. Fiasconaro, H. Q. Song, G. Giansiracusa, and U. Lombardo, Phys. Rev. C **65**, 017303 (2001).
[44] A. Lejeune and C. Mahaux, Nucl. Phys. A **295**, 189 (1978)
[45] R. B. Wiringa, V. G. J. Stoks, and R. Schiavilla, Phys. Rev. C **51**, 38 (1995).
[46] B. H. J. McKellar and R. Rajaraman, Phys. Rev. C **3**, 1877 (1971).
[47] D. W. E. Blatt and B. H. J. McKellar, Phys. Rev. C **11**, 614 (1975).
[48] A. Carbone, A. Polls, and A. Rios, Phys. Rev. C **88**, 044302 (2013).
[49] A. Carbone, A. Cipollone, C. Barbieri, A. Rios, and A. Polls, Phys. Rev. C **88**, 054326 (2013).
[50] B. D. Day, Phys. Rev. **151**, 826 (1966).
[51] R. Malfliet, Prog. Part. Nucl. Phys. **21**, 207 (1988).
[52] T. Cheon and E. F. Redish, Phys. Rev. C **39**, 331 (1989); R. Sartor, *ibid.* **54**, 809 (1996); K. Suzuki, R. Okamoto, M. Kohno, and S. Nagata, Nucl. Phys. A **665**, 92 (2000); F. Sammarruca, X. Meng, and E. J. Stephenson, Phys. Rev. C **62**, 014614 (2000).
[53] B. D. Day, Rev. Mod. Phys. **39**, 719 (1967).
[54] M. Baldo, I. Bombaci, L. S. Ferreira, G. Giansiracusa, and U. Lombardo, Phys. Lett. B **209**, 135 (1988); M. Baldo, I. Bombaci, L. S. Ferreira, G. Giansiracusa, and U. Lombardo, **215**, 19 (1988).
[55] B. E. Vonderfecht, W. H. Dickhoff, A. Polls, and A. Ramos, Nucl. Phys. A **555**, 1 (1993).
[56] B. E. Vonderfecht, W. H. Dickhoff, A. Polls, and A. Ramos, Phys. Rev. C **44**, R1265 (1991).
[57] P. Yin, J. Y. Li, P. Wang, and W. Zuo, Phys. Rev. C **87**, 014314 (2013).

[58] J. Carlson, V. Pandharipande, and R. Wiringa, Nucl. Phys. A **401**, 59 (1983).
[59] P. Grangé, J. Cugnon, and A. Lejeune, Nucl. Phys. A **473**, 365 (1987).
[60] M. Baldo, I. Bombaci, G. Giansiracusa, and U. Lombardo, Nucl. Phys. A **530**, 135 (1991).
[61] O. Benhar, A. Fabrocini, and S. Fantoni, Nucl. Phys. A **505**, 267 (1989); Phys. Rev. C **41**, R24 (1990).